JOURNAL OF OPTOELECTRONICS AND ADVANCED MATERIALS, Vol. 10, No. 9, September 2008, p. 2237 - 2243

Comparative study of hybrid nanostructures of polymer-magnetic nanoparticles

R. TURCU*, A. NAN, I. CRACIUNESCU, J. LIEBSHER[a], O. PANA, D. BICA[b], L.VEKAS[b], C. MIJANGOS[c]
National Institute for Research and Development of Isotopic and Molecular Technologies, P.O.Box 700, Cluj-Napoca 5, 400293 Romania
[a] *Institut fur Chemie, Humbold-Universitat Berlin, 12489 Berlin*
[b] *Romanian Academy, Timisoara Branch, Magnetic Fluids Laboratory, Timisoara, Romania*
[c] *Instituto de Ciencia y Tecnología de Polímeros, CSIC, 28006 Madrid, Spain*

In this work we focus on the hybrid nanostructures magnetic-polymer obtained by the combination of Fe_3O_4 ferrofluid (FF) with either a conducting polymer like polypyrrole (PPy) or an insulating polymer like polyvinyl alcohol (PVA). Magnetic composites with different morphology were obtained: (i) as core-shell nanostructures with Fe_3O_4 as the magnetic core and PPy as the shell; (ii) as ferrogels, by the dispersion of Fe_3O_4 nanoparticles into PVA matrix. The novel core-shell hybrid nanostructures, consisting in the deposition of a conjugated polymer shell (polypyrrole or functionalized pyrrole copolymers) covering the magnetic core were prepared by chemical oxidative polymerization of the monomer in aqueous solution containing the ferrofluid. Several synthesis parameters (oxidant/monomer ratio, unsubstituted pyrrole/substituted pyrrole ratio, magnetic nanofluid/monomer ratio, polymerization time) were varied in order to tailor the properties of magnetic-copolymer nanocomposites. The synthesis of PVA ferrogels has been carried out mixing corresponding amounts of Fe_3O_4 ferrofluid and aqueous PVA solution. The properties of the magnetic-polymer hybrid nanostructures were investigated by TEM, HRTEM, FTIR spectroscopy, thermogravimetric analysis (TGA) and magnetization measurements. A comparative study of the nanostructure-properties relationship for hybrid magnetic-polymer composites prepared in different synthesis conditions is reported.

(Received February 25, 2008; accepted August 14, 2008)

Keywords: Conducting polymer, Magnetic nanoparticles, Hybrid nanostructures.

1. Introduction

The association of polymers with magnetic nanoparticles represents a very promising route to obtain nanostructured composites with novel properties difficult to get from the individual components. The achievement of a hybrid system magnetic nanoparticle – polymer allows also the functionalization and the control of the magnetic nanoparticle properties by the specific composition of the polymer [1, 2]. There is an increasing interest for magnetic-polymer nanocomposites from both fundamental and applicative point of view, these materials being potential candidates for different applications including biomedicine, magnetic recording media, spin-polarized devices, electromagnetic shielding, biosensors, catalytic uptake of pollutants, magnetic separation [1-3].

The recent research efforts dedicated to the development of polymer based magnetic nanostructures can be grouped as follows: i) the achievement of different magnetic nanoparticles with controlled morphology and magnetic properties; ii) embedding the magnetic nanoparticles into polymeric matrices or obtaining the core-shell structures with a magnetic core covered by a polymer shell.

Different types of magnetic nanoparticles have been used to obtain magneto-polymer composites: iron oxides as Fe_3O_4 and γ-Fe_2O_3 [4, 5], CoNi [6], $ZnFe_2O_4$ [7] and $CoFe_2O_4$ [8, 9]. Ferrofluids represent a special category of smart nanomaterials, consisting of stable dispersion of magnetic nanoparticles in different liquid carriers. Stabilization of ferrofluid implies various procedures depending on the nature of the liquid [8].

The dispersion of solid nanoparticles within a polymeric matrix can be used to stabilize, isolate and characterize the magnetic nanoparticle [10]. A key problem is the homogeneous dispersion of the magnetic nanoparticles in the polymeric matrix. Polymers with a tridimensional structure, especially chelating resins, such as poly(vinyl alcohol) (PVA), poly(vinyl chloride) (PVC), polystyrene, polyimide or conducting polymers have been used to obtained magnetic nanocomposites [10-12]. Polymeric gels are very attractive systems as a continuous medium in the preparation of uniformly dispersed magnetic polymer nanomaterials. Magnetic nanogels of common interest are ferromagnetic magnetite nanoparticles (Fe_3O_4) embedded into a cross-linked polymer.

Among conducting polymers, polypyrrole (PPy) was intensively used in association with magnetic nanoparticles like F_2O_3, Fe_3O_4 to get nanocomposites by using different synthesis methods [11-18]. Different surfactants and oxidants can be used for the magnetic nanoparticles stabilization and for the pyrrole polymerization process and as a consequence, the

properties of the composites differ with the synthesis conditions. Therefore, the improvement of the nanocomposites characteristics in order to design a specific application requires a deeper understanding of the effects induced by the synthesis parameters.

We have already studied the polypyroll-carton nanotubes hubrid materials [19].

In the present work we focus on the hybrid nanostructures magnetic-polymer obtained by the combination of Fe_3O_4 ferrofluid (FF) with either a conducting polymer like functionalized polypyrrole (PPy) or an insulating polymer like polyvinyl alcohol (PVA). Magnetic composites with different morphology were obtained: (i) as core-shell nanostructures with Fe_3O_4 as the magnetic core and PPY as the shell; (ii) as ferrogels, by the dispersion of Fe_3O_4 nanoparticles into PVA matrix. The nanocomposites structural, optical and magnetic properties were investigated by TEM, HRTEM, FTIR spectroscopy, thermogravimetry (TGA) and magnetization measurements. Our main goal is to gain insight into the correlations between the synthesis parameters and the physical properties of the polypyrrole-magnetic nanocomposites in order to control the characteristics for specific applications.

2. Experimental

Samples preparation

Fe_3O_4 water based ferrofluid (FF) was obtained by chemical coprecipitation followed by double layer steric and electrostatic stabilization of magnetite nanoparticles in water carrier liquid. Combinations of surfactants with different chain lengths myristic acid (MA) and dodecyl-benzene-sulphonic acid (DBS) were used, such as DBS+DBS and MA+DBS [8].

The pyrrole monomer with attached functional group, 3-(1-Pyrrolyl)propanoic acid (Fig.1) was prepared according to known literature procedures [20, 21].

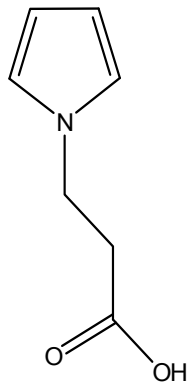

Fig. 1. 3-(1-Pyrrolyl)propanoic acid.

The magnetic nanocomposites based on polypyrrole were prepared by the oxidative polymerization of pyrrole monomer (Py) in aqueous solution containing an oxidant, ammonium peroxodisulfate (APS) and water based ferrofluid [3, 11]. The functionalized magnetic nanocomposites were obtained by oxidative polymerization of substituted pyrrole (3-(1-Pyrrolyl)propanoic acid) and unsubstituted pyrrole in aqueous solution containing APS as oxidant and the ferrofluid. The reactions proceeded at room temperature under magnetic stirring for 10h. The reactions were terminated by adding excess methanol to the reaction flask. The resulting black precipitate was separated by centrifugation, washed with water and dried at 60^{o}C for 24 h. The synthesis parameters for magnetic nanocomposites based on polypyrrole (samples iPPy-FF, i=1, 2, 3) and functionalized pyrrole copolymer, respectively (samples icoPPy-FF, i=4, 5, 6) are given in Table 1.

The synthesis of PVA-Fe_3O_4 ferrogels has been carried out mixing corresponding amounts of Fe_3O_4 ferrofluid and aqueous PVA solution 10 wt%. PVA solution was prepared in hermetic Pyrex tubes by mixing the appropriate amount of polymer and water (milliQ grade) at 90°C under continuous stirring until the polymer was completely dissolved. After adding the corresponding amount of ferrofluid, the final solution was poured into a cylindrical mold and it was frozen by cooling for 30 minutes. After this time, the solution was allowed to thaw at room temperature for 30 min. Chemical cross linking reaction of the mixed solution was achieved by 5 freezing-thawing (F-T) cycles. After the corresponding F-T cycles, samples were left in water until swelling equilibrium. The synthesis conditions for the PVA- Fe_3O_4 ferrogels are given in Table 2.

Table 1. The synthesis parameters for magnetic nanocomposites based on polypyrrole and functionalized pyrrole copolymer.

Sample	Ferrofluid	FF/Py (v/v)	APS/Py (M)	Polym. time (h)
1PPy-FF	Fe_3O_4 /DBS+DBS	20	0.2	10
2PPy-FF	Fe_3O_4 /DBS+DBS	10	0.2	10
3PPy-FF	Fe_3O_4 /MA+DBS	20	0.2	10
4coPPy-FF*	Fe_3O_4 /MA+DBS	10	0.5	10
5coPPy-FF**	Fe_3O_4 /MA+DBS	10	0.2	24
6coPPy-FF**	Fe_3O_4/ DBS+DBS	10	0.5	10

* The ratio Py/substituted Py= 1/5
** The ratio Py/substituted Py= 1/3

Characterization methods

The morphology of the magnetic nanoparticles and PPy based magnetic nanocomposites was determined by TEM and HRTEM using 1010 JEOL and Hitachi H9000NAR transmission electron microscopes. Infrared absorption spectra were recorded by a spectrophotometer JASCO FTIR-6100, on pressed pellet prepared from the nanocomposites powder embedded in KBr, the range 400-4000 cm^{-1} spectral range. Elemental analysis of the nanocomposites samples were performed by a LECO CHNSFe – 932 apparatus. Dynamic thermal degradation measurements on PVA and PPy nanocomposites were performed in a TA TGAQ500 Analyzer. Runs were performed in dynamic mode in nitrogen from 25 to 700°C at 10°C/min. All the nanocomposite samples were dried to constant weight prior to be investigated by TGA. The magnetic measurements were performed at room temperature by using a Vibrating Sample Magnetometer DMS 880.

Table 2. The synthesis parameters for PVA- Fe_3O_4 ferrogels

Sample	Ferrofluid	PVA conc. (wt %)	Fe_3O_4 (wt %) (b)
1PVA-FF	Fe_3O_4 / MA+DBS	10	2
2PVA-FF	Fe_3O_4 /MA+DBS	10	1
3PVA-FF	Fe_3O_4 / MA+DBS	10	0.5
4PVA-FF	Fe_3O_4 / MA+DBS	10	0.25

3. Results and discussion

The TEM images of the ferrofluids stabilized with different combinations of surfactants are presented in the Figs. 2(a) and 2(b). The magnetite nanoparticles are almost spherical and their size distribution is influenced by the surfactant nature [25]. Based on TEM investigations we have already shown in [25] that the mean diameter of Fe_3O_4 nanoparticles stabilized with MA+DBS (6.9 nm) is smaller than that of Fe_3O_4 stabilized with DBS+DBS (8.2 nm). The mechanism of pyrrole polymerization is the radical cations coupling, the positive charges on the generated chain being compensated by the surfactants anions which stabilize the magnetite particle. Therefore, a core-shell structure with the magnetite covered by PPy shell is obtained. In the Fig. 3 one can observe the amorphous PPy layer (1-3 nm thickness) surrounding the crystalline magnetite nanoparticles. The HRTEM images of the magnetic nanocomposites based on functionalized pyrrole copolymer are given in the Figs. 4(a) and 4(b). It is worth to mention that for these nanocomposites it is more difficult to observe the core-shell structure as compared with that one based on PPy. This fact could be due to the more slowly polymerization rate of the substituted pyrrole as compared with unsubstituted pyrrole, which results in a lower thickness of the functionalized pyrrole copolymer layer onto the magnetite surface.

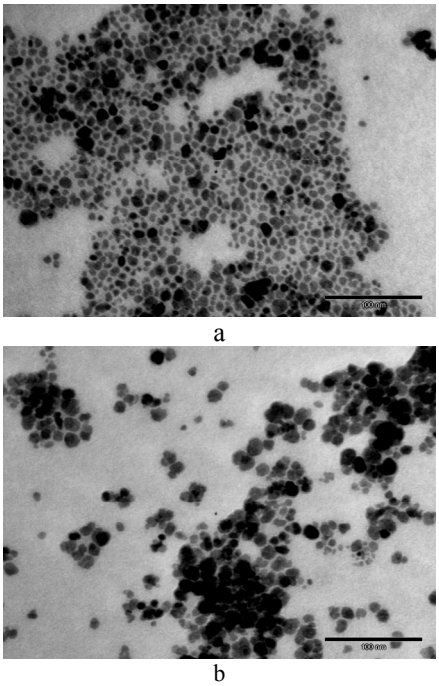

a

b

Fig. 2. TEM images of ferrofluids: (a) Fe_3O_4 /MA+DBS, (b) Fe_3O_4 /DBS+DBS.

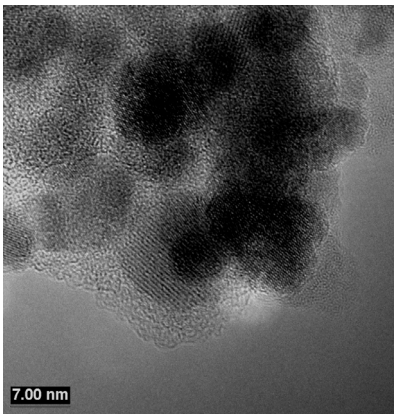

Fig. 3. HRTEM of the magnetic nanocomposites sample 1PPy-FF from Table 1.

The TEM image of PVA-Fe_3O_4 ferrogel (sample 4PVA-FF from Table 2) is shown in the Fig. 5. The observed partial agglomeration of the magnetic nanoparticles is due to TEM samples preparation process.

The formation of the magnetic nanocomposites based on polypyrrole and functionalized pyrrole copolymer is demonstrated by the presence of the characteristic absorption bands of the components in the FTIR spectra. Fig. 6 shows a comparison between the FTIR spectra of PPy doped with DBS and that ones of the nanocomposites prepared with the ferrofluid stabilized with different

surfactants, samples 1PPy-FF and 3PPy-FF from the Table 1. The FTIR spectra of the nanocomposites contain the characteristic absorption bands of oxidized PPy and the intense absorption band located around 570 cm^{-1} ascribed to Fe_3O_4 [21, 22]. Still some relevant differences appear between the spectra of the nanocomposites and that of PPy concerning the relative intensities and peak positions of the absorption bands. It is well known that the PPy absorption bands are sensitive to the oxidation level and to the conjugation length of the PPy chain [21].

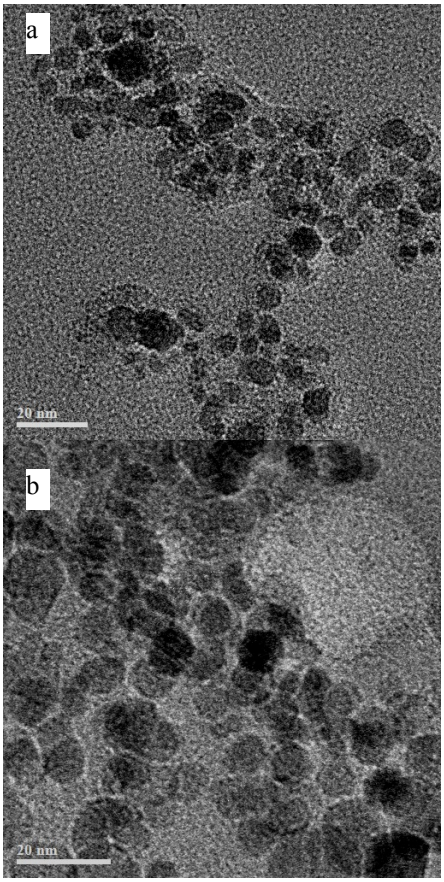

Fig. 4. HRTEM images of magnetic-pyrrole copolymer samples from table I: (a) 4 coPPy-FF; (b) 6 coPPy-FF**.*

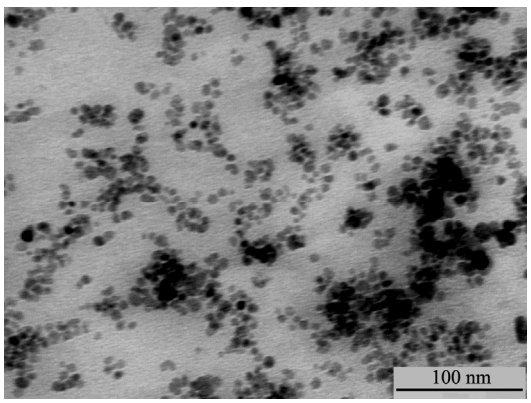

Fig. 5. TEM image of PVA ferrogel prepared with the ferrofluid Fe_3O_4 / MA+DBS.

Fig. 6 shows that the absorption bands characteristic for pyrrole ring vibrations, located at 914, 1198, 1465 cm^{-1} in the PPy spectrum, are significantly shifted to lower frequencies in the nanocomposites spectra. It indicates a higher degree of oxidation of the PPy shell which covers magnetite nanoparticles as compared with conventional PPy [24]. It is worth mentioning that the bands associated with in-plane C-H deformation vibrations in PPy have the same peak positions for all the spectra (1037 and 1300 cm^{-1}), suggesting that these vibrations are not sensitive to the oxidation level of PPy. Another interesting feature of the nanocomposites spectra from Fig. 6 is the shift to lower frequencies (1541-1543 cm^{-1}) of the absorption band ascribed to the collective vibration mode of intra-ring and inter-ring C=C/C-C, as compared to that in the spectrum for PPy (1553 cm^{-1}). The position of this band is related with the conjugation length of PPy chains [21]. The shift to lower frequencies indicates an increase of the conjugation length in the nanostructured thin PPy layer covering Fe_3O_4 nanoparticles as compared with conventional PPy.

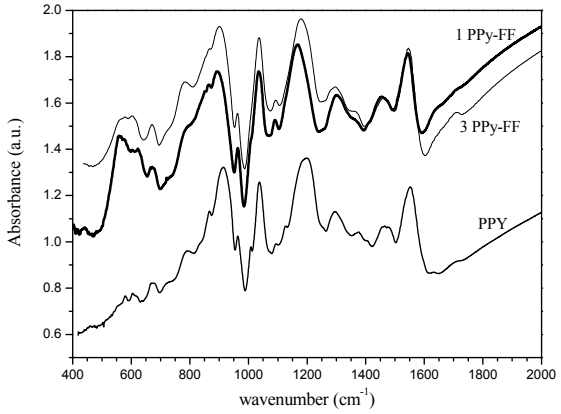

Fig.6. FTIR spectra of PPy doped with DBS and of PPy magnetic nanocomposites prepared with ferrofluids stabilized with different surfactants, samples from Table 1: 1PPy-FF (DBS+DBS), 3PPy-FF (MA+DBS).

In the Fig. 7 are given the FTIR spectra of polypyrrole and functionalized magnetic-copolymer samples. As expected, the strong absorption band ascribed to Fe_3O_4 appears in all the spectra of magnetic-copolymer samples. A new band located at 1705 cm^{-1}, characteristic to the C=O group appears in the spectra for the magnetic-copolymer samples in the Fig. 7. The observed changes of the absorption bands for the copolymers as compared to that ones for PPy are due to the chains conformational modifications induced by the attached functional group and can be correlated with the unsubstituted pyrrole/ substituted pyrrole ratio. The spectrum of the sample 4coPPy-FF, prepared with the higher amount of substituted pyrrole than sample 6coPPy-FF, shows more significant changes of the intensities and peak positions for the absorption bands characteristic for pyrrole ring vibrations, located at 914, 1198, 1465 cm^{-1} in the PPy spectrum. Besides the absorption band ascribed to the

collective vibration mode of intra-ring and inter-ring C=C/C-C shift to higher frequency in the spectrum of the sample 4coPPy-FF (1570 cm^{-1}) as compared to that in the spectrum of PPy (1550 cm^{-1}). The position of this band being correlated with the conjugation length of polymer chains [21], its shift to higher frequencies indicates a decrease of the conjugation length for the copolymer in the sample 4coPPy-FF as compared to PPy.

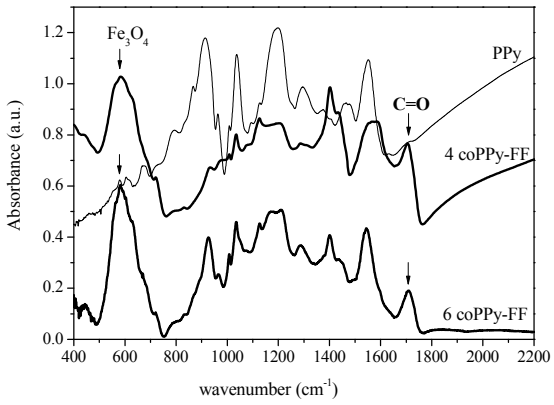

Fig. 7. FTIR spectra of polypyrrole and functionalized magnetic-copolymer nanocomposites, samples 4coPPy-FF and 6coPPy-FF from Table 1.

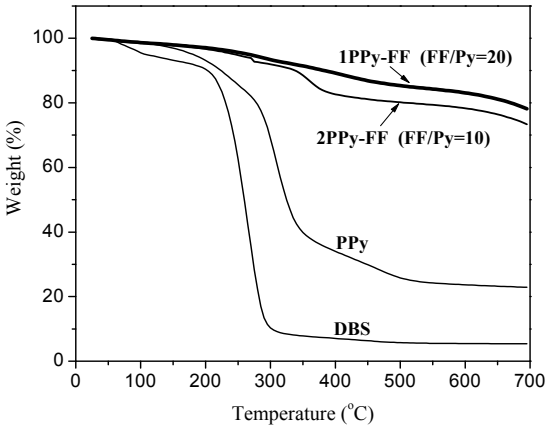

Fig. 8. Thermogravimetric curves for PPy doped with DBS and magnetic nanocomposites based on PPy, samples 1PPy-FF and 2PPy-FF from Table 1.

A comparison between the thermograms of PPy doped with DBS and that ones of PPy magnetic nanocomposites prepared at different FF/Py ratios, is shown in the Fig. 8. One can observe that the first weight loss process, in the temperature range 25-150°C, is independent of the samples composition and is associated with the loss of adsorbed water. The next weight loss processes in the temperature ranges 250-400°C and 550-650°C can be attributed to elimination of some volatile compounds, to splitting of the main chain of the surfactant and polymer decomposition respectively. These weight loss processes are influenced by the magnetite concentration used for nanocomposites preparation. From the Fig.8 one can observe that the thermal stability of PPy-magnetic nanocomposites prepared using ferrofluid is significantly improved as

compared with PPy. The interaction between PPy and Fe_3O_4 could be responsible for the increase of nanocomposites thermal stability.

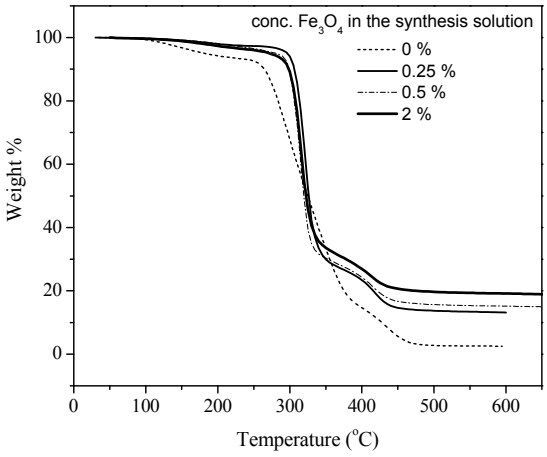

Fig. 9. Thermogravimetric curves for PVA-Fe_3O_4 ferrogels prepared with different concentrations of magnetite nanoparticles from the ferrofluid.

Fig. 9 shows that the thermal stability of PVA ferrogels is also improved by the addition of magnetic nanoparticles, but the effect is lower as compared with PPy-magnetic nanocomposites.

The first weight loss process for ferrogels is associated with loss of absorbed moisture and/or with the evaporation of trapped solvent. The second weight loss process corresponds to the degradation of PVA by a dehydratation reaction on the polymer chain [26]. The position of the associated decomposition temperature is shifted to higher temperature with increasing Fe_3O_4 content. The improvement of polymer stability may be related to the restriction in polymer chain mobility. In the third weight loss process, the polymer residues are further degraded at approximately 450 °C to yield carbon and hydrocarbons. The degradation temperature corresponding to this weight loss process depends of the Fe_3O_4 content. From the weight of the residues one can determine the Fe_3O_4 content of PVA ferrogels being in the range 10-16 % for the investigated samples, Fig. 12.

The magnetization curves at room temperature for PVA ferrogels (samples prepared in the conditions given in Table 2) with different concentrations of magnetite are presented in Fig. 10. The magnetization curves show no hysteresis, this behaviour being superparamagnetic. This means that the magnetite nanoparticles do not cluster during the ferrogel preparation. The magnetization of dry PVA ferrogels depends on the magnetite concentration. The values of the saturation magnetization, M_s are in the range 1.4-5.5emu/g, increasing with the content of magnetite.

A similar superparamagnetic behaviour of the magnetization at room temperature was obtained for

magnetic nanocomposites based on polypyrrole and functionalized pyrrole copolymer (Figs. 11 and 12). But one order of magnitude higher values for magnetization are obtained for PPy based nanocomposites as compared with PVA ferrogels. The results of elemental analysis show that a higher quantity of magnetite can be embedded during the pyrrole polymerization process as compared with that one in PVA ferrogels, resulting in higher magnetization values for PPy nanocomposites.

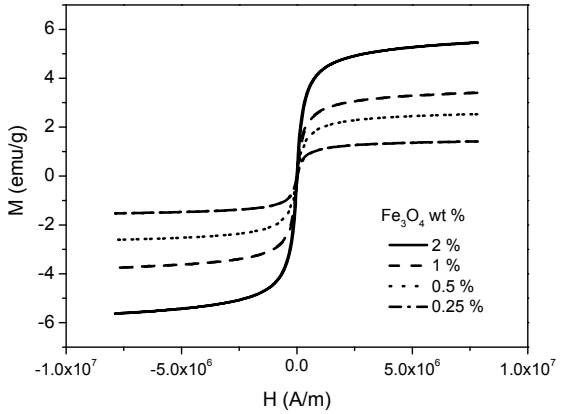

Fig. 10. Magnetization vs. applied magnetic field at room temperature for PVA ferrogels (samples from Table 2) prepared with different magnetite concentrations.

From the Fig.11 one can see that for the PPy magnetic nanocomposites prepared with the same ratio APS/Py=0.2 and the same polymerization time (10 h), the value of M_S depends on the ratio FF/Py in the synthesis solution: 1PPy-FF (FF/Py=20), M_S= 43 emu/g; 2PPy-FF (FF/Py=10), M_S=38 emu/g. The oxidant/monomer ratio and polymerization time are relevant synthesis parameters that allow tailoring the magnetic properties of the magnetic-polymer nanocomposites [3, 11].

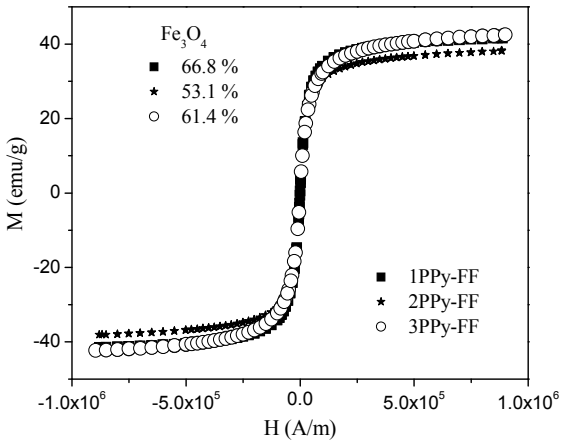

Fig.11. Magnetization vs. applied magnetic field at room temperature for PPy- magnetic nanocomposites (samples from Table 1) with different Fe_3O_4 concentrations as determined from elemental analysis.

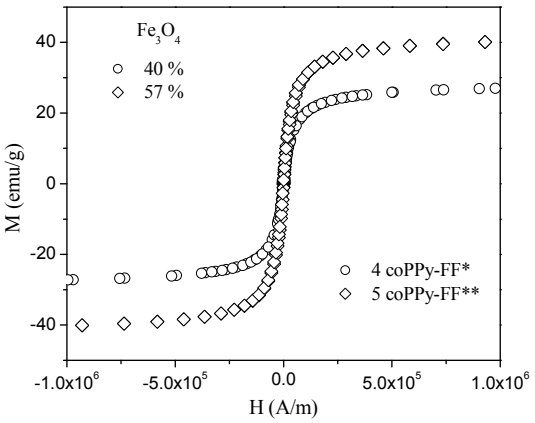

Fig.12. Magnetization vs. applied magnetic field at room temperature for magnetic nanocomposites based on functionalized pyrrole copolymer, (samples from Table 1) containing different Fe_3O_4 concentrations as determined from elemental analysis.

Fig. 12 shows that the magnetic-copolymer nanocomposite prepared at APS/Py=0.5 have a lower saturation magnetization (sample 4coPPy-FF* , M_S=28.5 emu/g) as compared with that one prepared at lower APS/Py ratio (sample 5coPPy-FF** , M_S=41.5 emu/g). The increase of oxidant/monomer ratio determines a high polymerization rate, resulting in an increase of the amount of polymeric component in the nanocomposite and consequently the mass magnetization decrease. From the Fig. 12 one can see that the magnetization vs. applied magnetic field for the functionalized magnetic nanocomposites based on pyrrole copolymer have no hysteresis. The relatively high magnetization values, the superparamagnetic behaviour and the biocompatibility of polypyrrole make this functionalized magnetic – copolymer nanocomposites promising materials for biomedical applications.

4. Conclusions

Magnetic-polymer nanocomposites were obtained by the combination of Fe_3O_4 ferrofluid (FF) with either a conducting polymer like polypyrrole (PPy) or an insulating polymer like polyvinyl alcohol (PVA). The double layer sterical stabilization of Fe_3O_4 nanoparticles with different surfactants combinations (MA+DBS, DBS+DBS) allows the pyrrole polymerization around the magnetic nanoparticles. A core-shell structure was obtained with the magnetite core covered by the polypyrrole or functionalized pyrrole copolymer. The surfactants layer avoids the aggregation of magnetic nanoparticles resulting in their good dispersion in the PVA matrix.

The thermal stability of the magnetic-polymer nanocomposites is influenced by the Fe_3O_4 content. The improvement of PVA ferrogel stability may be related to the restriction in polymer chain mobility. The increase of the magnetite content results in a significant increase of the thermal stability of the nanocomposites based on

polypyrrole. This effect could be attributed to the interaction between polypyrrole and magnetic nanoparticles.

The magnetic properties of the magnetic-polymer nanocomposites tailored as a function of magnetite content. The superparamagnetic behavior of magnetite nanoparticles in the investigated nanocomposites was evidenced by the missing hysterezis loop in the magnetization vs. applied magnetic field dependences.

These magnetic nanocomposites based on PVA or PPy have great potential for applications in biomedicine.

Acknowledgments

We acknowledge fruitful collaboration with Prof. O. Chauvet and Dr. Eric Gautron in the framework of PAI Brincusi 08868VB / 2005. This work was supported by the Romanian Ministry of Education and Research under the research programs, CEEX-MATNANTECH project nr. 12/2005, CEEX-CNMP project nr. 208/2006.

We acknowledge the participation in the EU NoE Nanofun-Poly, FP6-500361-2.

References

[1] J. Rodriguez, H. J. Grande and T. F. Otero, Handbook of Organic Conductive Molecules and Polymers, Ed. H S Nalwa, John Wiley & Sons, 1997, p 453.
[2] R. Gangopadhyay, A. De, Chem. Mater. **12,** 608 (2000).
[3] R. Turcu**,** O. Pana, A. Nan, L. M. Giurgiu, Polymeric Nanostructures and Their Applications vol 1, Ed. H.S. Nalwa, American Scientific Publishers, p. 337 (2007).
[4] Y. Xiaotun, X. Lingge, N. S. Choon, C. S. On Hardy, Nanotechnology **14**, 624 (2003).
[5] D.Y. Godovsky, A.V. Varfolomeev, G.D. Efremova, V.M. Cherepanov, G.A. Kapustin, A.V. Volkov, M.A. Moskvina, Adv. Mater. Opt. Electron. **9**, 87 (1999).
[6] R. Sanz, C. Luna, M. Hernandez-Velez, M. Vázquez, D. Lopez, C. Mijangos, Nanotechnology **16**, 278 (2005).
[7] G.F. Goya, H.R. Rechenberg, J.Magn.Magn.Mater., **197**, 191 (1999).
[8] D. Bica, L. Vekas, M. Rasa, J.Magn.Magn.Mater., **252**, 10 (2002).
[9] E. Goiti, R. Hernandez, R. Sanz, D. Lopez, M. Vazquez, C. Mijangos, R. Turcu, A. Nan, D. Bica , L. Vekas, J. Nano. Polym. Nanocompos. **2,** 5 (2006).
[10] M. Breulmann, H. Coelfen, H.P. Hentze, M. Antonietii, D. Walsh, S. Mann, Adv. Mater., **10,** 237 (1998).
[11] R. Turcu, D. Bica, L. Vekas, A. Nan, D. Macovei, N. Aldea, O. Pana, O. Marinica, R. Grecu, C.V.L. Pop, Rom. Rep. Phys., **58**(3), 359 (2006).
[12] G. Bidan, O. Jarjayes, J. M. Frouchart and E. Hannecart, Adv. Mater., **6,** 152 (1994).
[13] O. Jarjayes, H. Fries, G. Bidan, Synth. Met. **69,** 343 (1995).
[14] M. T. Nguyen and A. Diaz, Adv. Mater., **6,** 858 (1994).
[15] F. Yan, G. Xue, J. Chen, Y. Lu, Synth. Met., **123,** 17 (2001).
[16] J. Liu and M. X. Wan, J. Polym. Sci. Part A: Polym. Chem., **38,** 2734 (2000).
[17] K. Sunderland, P. Brunetti, L. Spinu, J. Fanga, Z. Wang, W. Lu, Mater. Lett., **58** 3136 (2004).
[18] K. Suri, S. Annapoorni, R. P. Tandon and N. C. Mehra, Synth. Met., **126,** 137 (2002).
[19] R. Turcu, Al. Darabont, A. nan, N. Aldea, D. Macovei, D. Bica, L. Vekas, O. Pana, M. L. Soran, A. A. Koos, L. P. Biro, J. Optoelectron. Adv. Mater. **8**(2), 643 (2006).
[20] R. C. Blume, H. G. Lindwall, J. Org. Chem. **10,** 255 (1945).
[21] A. Guiseppi, A. M. Wilson, J. M. Tour, T. W. Brockmann, P. Zhang, D. L Allara, Langmuir 11, 1768 (1995).
[22] G. B. Street, Handbook of Conducting Polymers vol.1, Ed. T. A. Skotheim, New York Marcel Dekker, p. 279 (1986).
[23] F. F. Bentley, L. D. Smithson and A. L. Rozek, Infrared Spectra and Characteristic Frequencies 700-300 cm^{-1}, Interscience Publishers, John Wiley & Sons, p. 1528 (1968).
[24] G. Zerbi, M. Gussoni and C. Castiglioni, Conjugated Polymers, Ed. J.L.Bredas and R.Silbey, Kluwer Academic Publishers p. 435 (1991).
[25] R. G. Davidson and T. G. Turner, Synth. Met. **72,** 121 (1995).
[26] R. Turcu, A. Nan, I. Craciunescu, S. Karsten, O. Pana, I. Bratu, D. Bica, L. Vekas, O. Chauvet, D. Eberbeck, H. Ahlers, J. Nano. Polym. Nanocompos. **3**, 55 (2007).
[27] D.López, I. Cendoya, F.Torres, J.Tejada, and C. Mijangos, J. Appl. Polym. Sci., **82,** 3215 (2001).

*Corresponding author: rodicat14@yahoo.com